Introducing electron correlation in solid-state calculations for superconducting states

Wilver A Muriel, Trinidad Novoa, Carlos Cárdenas, Julia Contreras-García

Introducing electron correlation in solid state calculations for superconducting states

Wilver A. Muriel,[†,‡] Trinidad Novoa,[¶,§] Carlos Cárdenas,[†,‡] and Julia Contreras-García[*,¶]

†*Departamento de Física, Facultad de Ciencias, Universidad de Chile, Chile.*

‡*Centro para el Desarrollo de la Nanociencia y la Nanotecnología (CEDENNA), RM 9170124, Santiago, Chile*

¶*Laboratoire de Chimie Théorique, Sorbonne Université & CNRS, 4 Pl. Jussieu, 75005, Paris, France*

§*Laboratoire Jacques-Louis Lions, Sorbonne Université & CNRS, 4 Pl. Jussieu, 75005, Paris, France*

E-mail: contrera@lct.jussieu.fr

Abstract

Analyzing the electronic localization of superconductors has been recently shown to be relevant for understanding their critical temperature [Nature Communications 12, 5381 (2021)]. However, these relationships have only been shown at the Kohn-Sham DFT level, where the on-set of strong correlation linked to the superconducting state is missing. In this contribution, we approximate the superconducting gap in order to reconstruct the superconducting one-reduced density matrix (1RDM) from a DFT calculation. This allows us to analyse the electron density and localization in the strong correlation regime. The method is applied to two well known superconductors. Electron localization features along the electron-phonon coupling directions and hydrogen

cluster formations are observed for different solids. However, in both cases we see that the overall localization channels are not affected by the on-set of superconductivity, explaining the ability of DFT localization channels to characterize the superconducting ones.

Introduction

In the last years, there has been growing interest in hydrogen-rich materials due to their potential as high-temperature superconductors. H_3S[1], YH_6[2], LaH_{10}[3] and YH_9[4] have been demonstrated to reach critical temperatures, T_c, all above 200 K at megabar pressures. However, one of the great challenges of modern condensed-matter theory is the prediction of material-specific properties of superconductors, such as the critical temperature, T_c, and the gap at zero temperature, Δ. The model of Bardeen, Cooper, and Schrieffer (BCS) accounts for the universal behavior of all conventional superconductors, but it is not able to describe material dependent properties[5]. A major step in the first-principles approach to superconductivity is Eliashberg theory[6]. This method describes the effects of electron-phonon coupling very accurately. However, the treatment of Coulomb correlations is much harder, so that the electron-electron repulsion is usually introduced by means of an adjustable parameter μ^*, chosen to reproduce the experimental T_c[7,8].

Combining good accuracy with moderate numerical effort, density functional theory (DFT) is the method of choice for ab initio calculations of macroscopic properties in the weak correlation regime. Following the discovery of high-temperature superconductors, the formal framework of DFT has been generalized to describe strong correlation in the superconducting state[9]. Compared to traditional many-body approaches, superconducting DFT (SC-DFT) is absent of empirical parameters. Moreover, given its low computational cost, it has enabled the study of the full k-dependent anisotropy in the superconducting gap. In SC-DFT, the superconducting gap is estimated by doing a connection with Eliashberg theory, formulated in terms of Green's functions , and solving a self-consistent equation[9–13].

Unfortunately, this procedure is very complex and there are no simple computational tools developed for this purpose available to the public at this moment.

As a faster and alternative approach for predicting T_c, some of the authors have recently shown that the localization/delocalization pattern of a structure correlates with the critical temperature[14]. Nevertheless, this quantity has only been analyzed for the normal state (NS) (and conclusions extended to the superconducting one). In order to better understand its ability to reveal T_c, it would be necessary to analyze these delocalization channels in the superconducting state (SC). A first step in this direction has been recently put forward for a model Hamiltonian (1D tight-binding hydrogen chain)[15]. It was thence shown that the effect of the SC Hamiltonian is a temperature-resilient redistribution of the electrons over the base of the Kohn-Sham (KS) orbitals. Making use of this fractional occupations, the authors could propose a reformulation of the electron localization function for superconducting states.[15]

Along this contribution we will overcome the full self-consistent solution of the SC-DFT equations by making use of an approximated BCS occupation numbers in order to approximate the electron density matrix and electron localization function from a Kohn-Sham calculation. This will allow us to grasp electron reorganization introduced from correlation in well-known superconductors at the DFT-level cost.

Theoretical background

The Electron Localization Function (ELF) was first introduced by Edgecome and Becke to identify regions of localized same-spin electron pairs, or groups of them, in atomic and molecular systems.[16] Its original definition is based on the same-spin pair probability as approximated at the Hartree-Fock level. However, a more useful definition was later introduced by Savin[17] as the excess of local kinetic energy density (KED) due to Pauli repulsion:

$$\tau_{rel}(\boldsymbol{r}) = \frac{\tau(\boldsymbol{r}) - \tau_{vW}(\boldsymbol{r})}{\tau_{TF}(\boldsymbol{r})} \tag{1}$$

where $\tau(\boldsymbol{r})$, is the positive definite KED of the system, and $\tau_{vW}(\boldsymbol{r})$[18] is its form in the von-Weizsacker approximation. For a 3D system, the Thomas-Fermi kinetic energy density takes the form $\tau_{TF}(\boldsymbol{r}) = \frac{3}{10}(3\pi^2)^{2/3}\rho(\boldsymbol{r})^{5/3}$.

Note that for representation reasons, τ_{rel} is usually inversed and rescaled, leading to the common expression of ELF, which varies in the [0,1] range:

$$\eta(\boldsymbol{r}) = \left[1 + \left(\frac{\tau_{rel}(\boldsymbol{r})}{\tau_{TF}(\boldsymbol{r})}\right)^2\right]^{-1}, \tag{2}$$

Because the von-Weizsäcker kinetic energy is exact for a bosonic system of the same density $\rho(\boldsymbol{r})$, the term τ_{rel} is a local measure of the excess kinetic energy due to the fermionic nature of the electrons, or what we call the Pauli kinetic energy density. If this is high, it means that electrons in those regions are not paired/localized and the ELF will be small.[19] If the kinetic energy density is not locally increased as an effect of the exclusion principle, in that case we say that electrons are localized, which will be reflected on a high value of the ELF.

Figure 1 provides an example for CH_3OH, where the different regions of electron localization are highlighted by an ELF isosurface: the cores, the C-O, C-H and O-H bonds, and the Oxygen lone pairs.

This function allows for the description of electron localization within normal DFT. However, in order to recover the effects of the superconducting state it is necessary to resort to alternative formulations which recover the strong correlation. Staying within the DFT framework, it is possible to resort to Superconducting DFT (SC-DFT)[9–13], which represents an adapted version of Density Functional Theory (DFT) tailored specifically for superconductors. SC-DFT has demonstrated remarkable accuracy in predicting the critical temperatures (T_c) of traditional superconductors, all without the need for empirical parameters. In order to recover the nature of the superconducting state, the Hamiltonian in SC-DFT incorporates external potentials that account for crucial aspects of superconductors: electron-phonon interaction and Cooper pairs (see S.I. for a more detailed description).

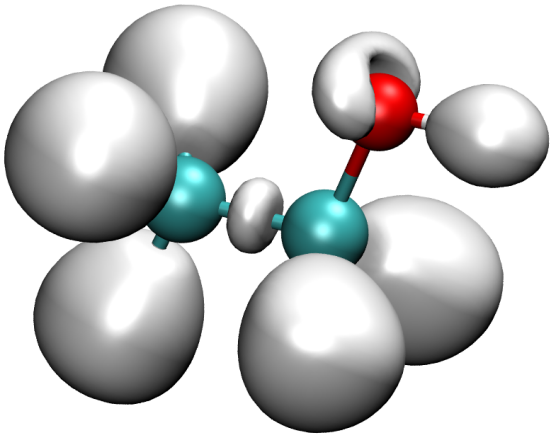

Figure 1: Isosurfaces of ELF= 0.85 of the CH_3OH molecule.

As recently introduced by some of the authors,[15] it is possible to approximately reconstruct the electron density and the kinetic energy densities of the superconducting state, as described in SC-DFT, in terms of the (normal state) KS natural orbitals, their energies, occupancies, the gap, and the temperature (see S.I.):

$$\rho^{SC}(\boldsymbol{r}) = \sum_{n\boldsymbol{k}} n^{SC}_{n\boldsymbol{k}} |\varphi_{n\boldsymbol{k}}(\boldsymbol{r})|^2 \,, \tag{3}$$

where

$$n^{SC}_{n\boldsymbol{k}} = 1 - \frac{\xi_{n\boldsymbol{k}}}{|E_{n\boldsymbol{k}}|} \tanh\left(\frac{\beta\,|E_{n\boldsymbol{k}}|}{2}\right). \tag{4}$$

where we have used the "SC" superscript to differentiate this density from the normal state (NS) electron density. Note that within this approach the orbitals energies E_{nk} take the form $E_{nk} = \sqrt{\xi^2_{nk} + \Delta_s(nk)^2}$, with $\Delta_s(nk)$ being the superconducting gap, and $\varphi_{nk}(r)$ and ξ_{nk} the Kohn-Sham orbitals and energies of the periodic system, respectively. Note that in

the normal state limit, $\Delta_s(nk) \to 0$, so that we recover the normal state density,

$$\rho^{NS}(\boldsymbol{r}) = \sum_{n\boldsymbol{k}} n^{NS}_{n\boldsymbol{k}} |\varphi_{n\boldsymbol{k}}(\boldsymbol{r})|^2. \tag{5}$$

where $n^{NS}_{n\boldsymbol{k}} = (1 + e^{\,\beta E_i})^{-1}$ is the Fermi-Dirac distribution. Hence, within the SC-DFT framework, we can express the difference in the electron densities when going from the normal to the superconductor state as a difference in the occupation numbers. Fractional occupation numbers is a necessary condition for a SC state as this is a superposition of states with different number of electrons (number symmetry breaking). However, it is not sufficient. Other correlations effects introduced by the pairing potential. Nevertheless, a similar approach to this have been proved to be useful to describe the correlation effects on the ELF in both, the ground[20] and excited states[21].

Similarly, it is possible to show that the positive definite KED of the superconducting state can be defined as,

$$\tau^{SC}(\boldsymbol{r}) = \frac{1}{2} \sum_{n\boldsymbol{k}} n^{SC}_{n\boldsymbol{k}} |\nabla_{\boldsymbol{r}} \varphi_{n\boldsymbol{k}}(\boldsymbol{r})|^2 \,. \tag{6}$$

The von Weizsacker and Thomas-Fermi approximations to the KEDs are obtained using $\rho^{SC}(\boldsymbol{r})$ from eq. (3),

$$\tau^{SC}_{vW}(\boldsymbol{r}) = \frac{1}{8} \frac{|\nabla_{\boldsymbol{r}} \rho^{SC}(\boldsymbol{r})|^2}{\rho(\boldsymbol{r})} \,, \tag{7}$$

and

$$\tau^{SC}_{TF}(\boldsymbol{r}) = \frac{3}{10} (3\pi^2)^{2/3} \, \rho^{SC}(\boldsymbol{r})^{5/3} \,, \tag{8}$$

respectively. Note that once again within this formalism, the differences between normal and superconducting states are expressed as changes in occupation numbers.

Finally, equations (6), (7), and (8) enable to define a superconducting ELF,

$$\eta^{SC}(\boldsymbol{r}) = \left[1 + \left(\frac{\tau^{SC}(\boldsymbol{r}) - \tau^{SC}_{vW}(\boldsymbol{r})}{\tau^{SC}_{TF}(\boldsymbol{r})}\right)^2\right]^{-1} . \tag{9}$$

This allows to analyze the spatial distribution of the electrons in a superconductor by means of the Electron Localization Function (ELF). In the same way as in the normal state, this function describes the localization patterns of the electrons in the superconducting state.

Hence, the superconducting ELF should help shine light on how the electrons arrange in the SC state, its similarities and differences with respect to the NS, and how this organization changes from one system to another. These equations have been applied to simple tight binding models[15], however, they have not been used to understand the electronic distribution in real solids so far. This is the aim of this contribution.

Computational approach

Within the SC-DFT approach, the difference between the spatial properties of the normal and the superconducting state lie exclusively on the occupation numbers of the KS orbitals (Eqs. 4 and 6). An approximated calculation of these SC occupation numbers will thus allow us to study the electron localization in superconducting states.

This approximation is based on the fact that it is possible to represent the dependence of the gap at zero Kelvin with respect to the energies ξ as an isotropic Lorentzian function:[22]

$$\Delta_0(\xi) = \frac{\Delta_0}{N_0\pi}\,\frac{\omega/2}{\xi^2 + (\omega/2)^2}\,, \tag{10}$$

where ω is a parameter that adjusts the width of the peak, and N_0 is a normalization such that the height of the peak at $\xi = 0$ is the gap at $T = 0$K in BCS, Taking into account the

dependence of the gap with respect to the temperature:

$$\Delta(T) = \Delta_0 \tanh\left(1.74\sqrt{\frac{T_c - T}{T}}\right). \tag{11}$$

we have a way to obtain the gap for a given T_c at any temperature.

Figure 2 offers the profile of the gap function for $\omega = 0.2$ eV at different temperatures, T, for the H_3S crystalline system assuming T_c=200K. These functions represent the width of the window around the Fermi energy where electrons will form Cooper pairs. One can see how the gap goes to zero everywhere when $T = T_c$. There, the properties of the normal and superconducting state become the same, as expected from SC-DFT.

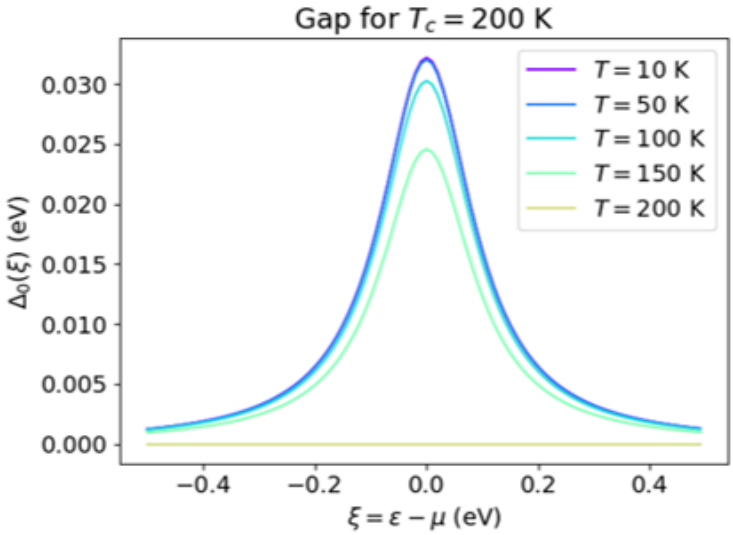

Figure 2: Gap function around the Fermi energy for $T_c = 200$ K. The dependence on the temperature T is shown by different colored lines.

Taking into account the gap in Fig. 2, the occupation numbers in the normal and superconducting states are those shown in Fig. 4. With this, it is possible to obtain the electron density and ELF of the superconducting state from a NS solid state calculation by a simple change in the fractional occupations. We have performed DFT calculations in well-known superconductor structures with the VASP package[23–26]. Geometries were relaxed using the Perdew–Burke-Ernzerhof[27] (PBE) functional. The same functional is used to compute the

electronic bands. The rapid oscillations of the inner shells of atoms were addressed with the projector augmented-wave method[28] with a kinetic energy cutoff of 600 eV. For integration on the reciprocal space, the first Brillouin zone was discretized with $32 \times 32 \times 32$ Monkhorst-Pack algorithm.

First we performed a self-consistent calculation of NS state at zero Kelvin and stored the Kohn-Sham Bloch states (WAVECAR file in VASP). Then we calculated the occupation numbers of the superconducting state for each band and each k-point with Eq. (4). The gap is considered to depend on the energy and the temperature according to Eqs. (10) and (11). Here we assumed that the same equation applies for all k-points and we fixed ω to 0.2 eV in order to fit the results obtained with SC-DFT in Ref.[29]. Finally, the superconducting state was prepared by reading these occupancies and applying them to the previously stored Kohn-Sham states. An accuracy in the occupation numbers of 10^{-3} was used, such that only those differing from 0 or 2 (normal state) by more than that threshold value were changed.

Two options were potentially possible: i) to use directly these Kohn-Sham states, or ii) to perform a self-consistent calculation (SCF) keeping the occupancies unaltered. In the latter case, special care must be taken to ensure that during the self-consistent procedure the labels of the KS states are not altered as this would result in an artificial change of the occupancies. For this purpose, we resorted to the VASP keywords $ALGO = Damped$ and $FERWE$. After a quick check, it was realized that although the ELF results were not affected by the convergence, densities were. Hence, the SCF (option ii) was kept. Applications to H_3S and LaH_{10} are analyzed in the coming section.

Applications

H_3S: a superconductor characterized by H-S interactions

This compound was synthetized and characterized at high pressure in 2015[30]. It has a H_3S stoichiometry above 100 GPa, with a T_c of ca. 200K at 150 GPa[30,31]

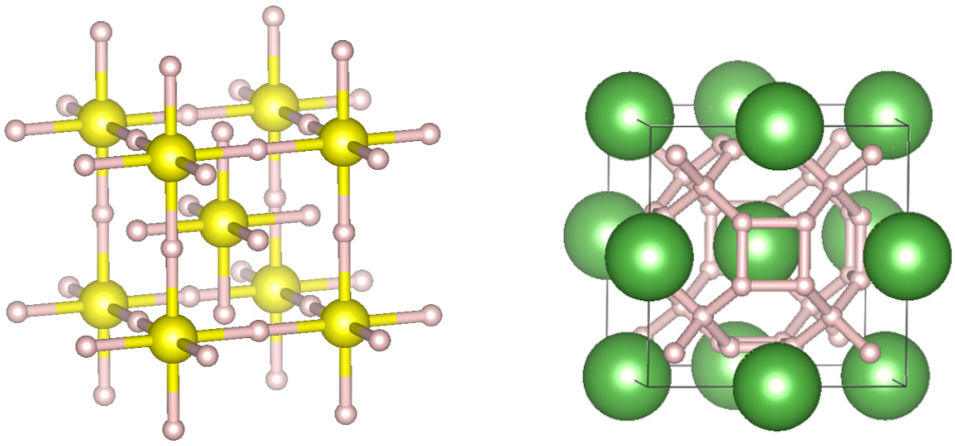

Figure 3: Left: H_3S with space group $Im\bar{3}m$ and lattice constant a_{cell}=3.07Å. Sulfur atoms occupy Wyckoff position $2a$ and H atoms occupy position $6b$. Right: LaH_{10} with space group $Fm\bar{3}m$, a_{cell}=4.42Å. La in position $4b$ and H in positions $8c$ and $32f$ (with x=0.1205).

The high pressure phase shows rhomboedral structure which can be approximated by a body-centred cubic (bcc) structure (at 150 GPa this means a change in the cell angle from 109.49° in the rhomboedral to 109.47° in the bcc)[32,33]. As shown in Fig. 3-left, the sulphur atoms occupy the corners of the cube as well as its centre, and the hydrogen atoms occupy the centre of the edges and faces of the cube.

Figure 4 allows to compare the occupation numbers for the metallic and the superconducting state resulting from the previous gap approximation. For a fixed critical temperature, it can be seen that the occupancies of the normal state deviate from the step function as the temperature increases, softening the transition around the Fermi energy. On the other hand, the superconducting occupation numbers do not suffer great alterations with the temperature. In fact, they tend to resemble the occupations at the critical temperature, showing the larger correlation of the superconducting state in comparison with the normal state below T_c. These occupations are temperature resilient.

If we analyze the electron density for the SC system at 10K (Fig. 5-left), we can see that non nuclear maxima appear in the direction of the S-H bonds[34]. The electron delocalization along these channels is also highlighted by the Electron Localization Function (Fig. 5-right). We can see how the region of electron localization around hydrogens stretches towards

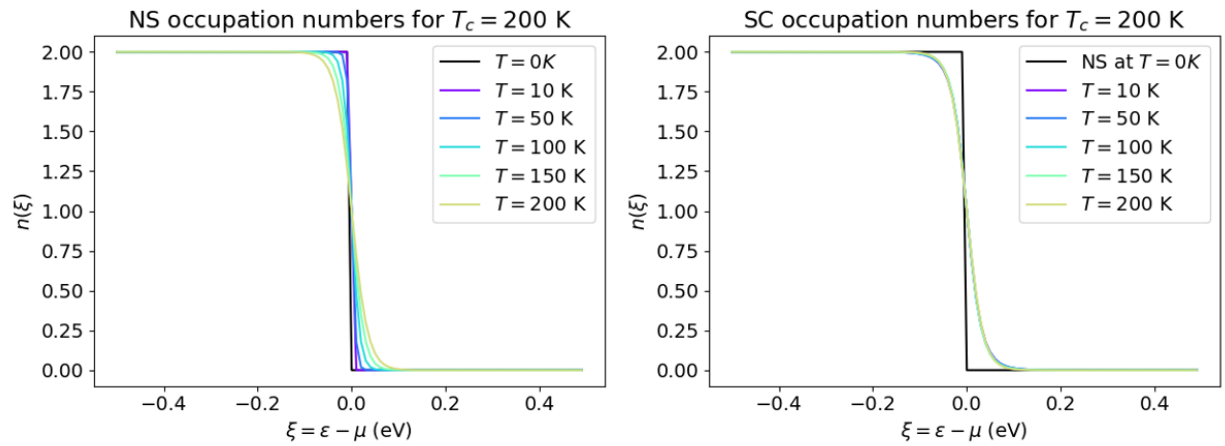

Figure 4: Occupation numbers at different temperatures for T_c=200K. To the left, the occupation numbers of the normal state, to the right, the same is displayed for the superconducting state. The normal state at $T = 0$ K is depicted in black.

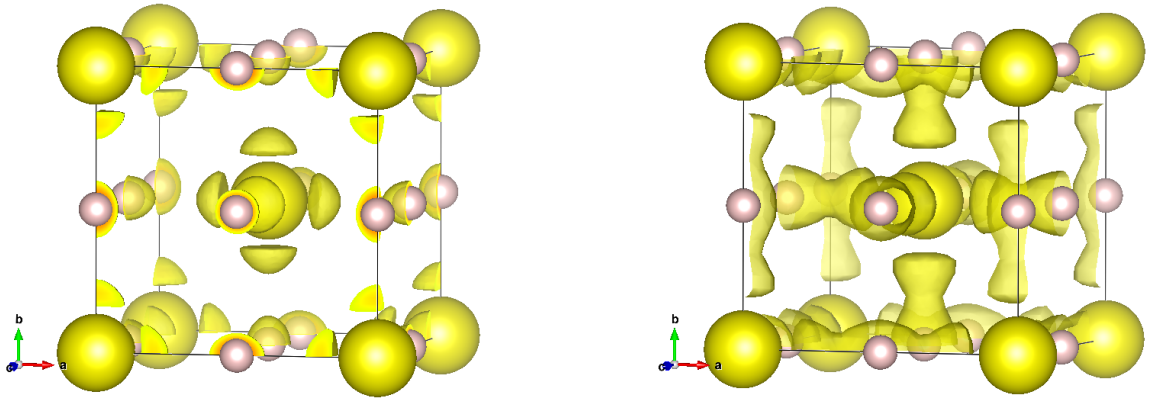

Figure 5: H_3S isosurfaces at T=10K. Left: ρ^{SC}=0.18 a.u. Right: $ELF^{SC} = 0.8$.

the sulfur atoms and leads to a localization region along the S-H direction in a "candy shape", as expected for an anionic hydrogen. Given the electron density build up in the S-H direction, the S-H interaction is strengthened and it is expected to behave anharmonically. This was already observed by Errea et al., who pinpointed that anharmonicity hardens the S-H stretching mode[35].

This picture is rather stable upon increasing the temperature (see T=200K in S.I.). In order to better visualize this difference, we have carried out a 3D grid difference of both scalar fields (Fig. 3 in S.I.). It can be seen that the differences appear mainly at the nuclei

and S-H bonding regions. However, interpretation of these data should be done with care. Differences are so small that they might be affected by numerical issues. Since the main differences are related to changes in population around the Fermi level (FL), we have thus decided to promote this information by the use of adapted formulae, which only focus in the FL region:

$$\rho_{FL} = \sum_{\boldsymbol{k}} n_\phi |\phi(\boldsymbol{k})|^2 \quad \forall \phi : n_\phi < 1.999 \text{ or } n_\phi > 0.001 \tag{12}$$

where FL makes reference to the fact that we are only calculating the quantity around the Fermi level, using thereto a criterion based on the fractional occupations (see Fig. 4 in S.I. for a visual depiction of the occupations). In order to verify that our implementation is working, we have carried out the integration of ρ_{FL} over the unit cell and compared to the integration of ρ. Whereas 18 electrons are obtained in the unit cell for the superconducting state at T=200K (6.137 electrons on S and 0.94-0.96 on hydrogens with a Bader partition); only 0.185 electrons are obtained when only the levels around the Fermi level are included (0.036 electrons on S and 0.018-0.019 electrons on hydrogen - note that compared to S, a bigger percentage of hydrogen charge is included in this integration as expected from the contribution of hydrogen atoms to the DOS[14]).

A similar FL criterion as in Eq. 12 is applied to the local quantities (kinetic energy densities) involved in the ELF definition. This allows us to focus on the correlated region of the superconductor. Results are shown for T=10K in Fig. 6. These new expressions allow to confirm the S-H direction as the one where correlation sets in, both from the ρ_{FL} and from the ELF_{FL} viewpoints. Noteworthy, important electron localization regions appear in the S-H direction (small "tear-like" features in Fig. 6-right).

Now, we can identify the main electronic reorganizations in the superconductor by plotting the same isosurface as we cool the superconductor from the critical temperature (200K) to very low temperatures (10K) (Fig. 7). Notice that, because in SC-DFT the superconducting state converges to the normal state at the critical temperature (where the gap goes to zero), ρ_{FL}^{200K} and ELF_{FL}^{200K}, which have been defined for superconducting state, also cor-

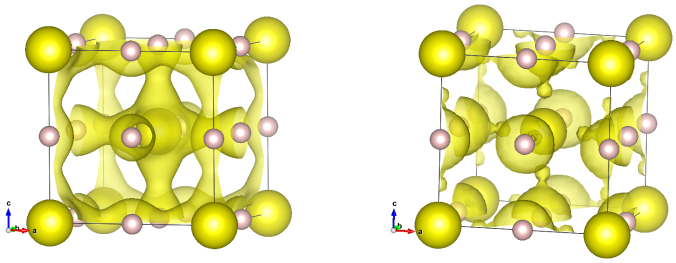

Figure 6: Electronic organization around the Fermi level at T=10K for H_3S. Left: ρ_{FL} = 0.0005 a.u. Right: $ELF_{FL} = 0.01$.

respond to the normal state quantities around the Fermi level at 200K.

Although the overall density values (ρ) do not change considerably with temperature (Fig. 7-left), those of ρ_{FL} do, as can be seen in Fig. 7-right.[1] Decreasing the temperature below T_c induces changes in the localization of electrons near the Fermi level, which is privileged around the S-H bond stretching direction. Similarly, the isosurfaces of the total ELF do not show any difference with the temperature, whereas those of ELF_{FL} do suffer some changes, while keeping a similar topology (see Fig. 5 in S.I.).

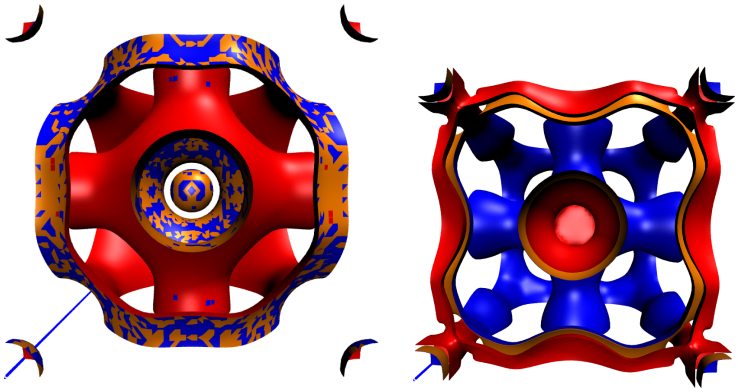

Figure 7: H_3S isosurfaces at 10K (blue), 100K (orange) and 200K (red). Left: ρ=0.08 a.u. Right: ρ_{FL}=0.0015 a.u.

[1]To understand why the isovalues of ρ_{FL} are taken to be as low as 0.01 a.u., one must take into account the total number of electrons in the energy window, of only 0.185.

LaH_{10}

In 2017, a systematic high pressure *ab initio* structural search performed revealed the stability of the LaH_{10} at high pressure under a fcc phase[36] and a very high coordination of La by hydrogen atoms (see Fig. 3-right). This structure was subsequently shown to have a critical temperature above 250K[3]. It is also worth noting that this compound is known to show very strong quantum effects.

Given the results for H_3S we will directly concentrate in the density and ELF around the Fermi level (Eq. (12)). Fig. 8 shows how the electron density where correlation takes place (ρ_{FL}) is mainly located around the hydrogen atoms instead of the bonds. Electron localization (ELF_{FL}) is also mainly centered in H atoms, with important delocalization channels in the H_4 units.

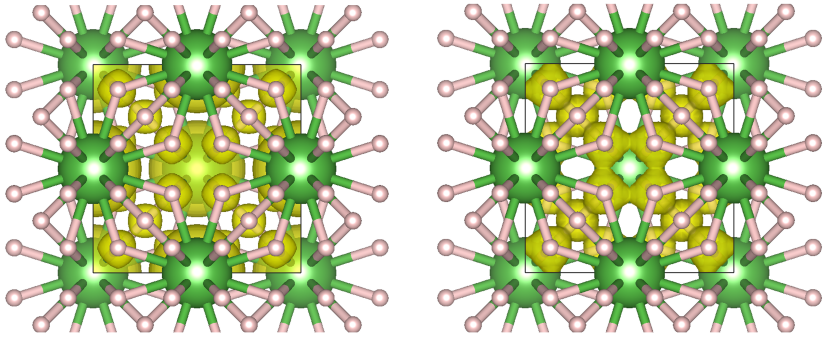

Figure 8: LaH_{10} isosurfaces around the Fermi surface at 10 K. Left: $\rho_{FL} = 0.0008$ a.u. Right: $ELF_{FL} = 0.001$.

The isosurfaces of the overall density show, once again, a temperature-independent character (see Fig. 9-left). On the other hand, while the isosurfaces of ρ_{FL} in Fig. 9-right have a similar shape, they do evidence some small changes in their values leading to a square pattern. Those differences become more important with the decrease of temperature in the atomic sites inside the H_4 units, revealing the change of character of the electrons in that region below T_c, when the system is in the superconducting regime.

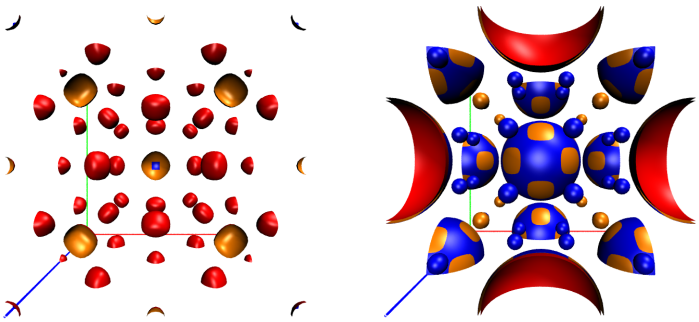

Figure 9: LaH_{10} isosurfaces at 10K (blue), 100K (orange) and 250K (red). Left: ρ=0.08 a.u.; Right: ρ_{FL}=0.0015 a.u.

Localization channel topologies

Overall, no big changes have been observed on the full electron density and ELF. Hence, we have also analyzed their critical points both for for H_3S and LaH_{10} at different temperatures. We are specially interested in saddle points, since the values of ELF at some of these points have been correlated to Tc in Ref.[14]. Looking at Fig. 9 in S.I., it can be seen that the saddle point position and ELF values are extremely stable upon the changes in the fractional occupation changes given by Eq. 4. This confirms the possibility of using the normal state to characterize the delocalization of the SC state and hence the equation that correlate Tc with delocalization channels.

Conclusions

Making use of the recently introduced SC-ELF, which allows to calculate the Electron Localization Function for a superconducting state as provided by SC-DFT,[15] we have introduced an approximation to calculate it from NS-DFT. By approaching the SC gap by a Lorentzian function, it was possible to calculate the expected occupations for a given gap, T_c and T. Hence, the SC electron localization can be obtained from a common solid state calculation, where correlation is introduced as a redistribution of electrons around the Fermi level. We have applied this approach to two typical superconductors, H_3S and LaH_{10}. Given the fact

that the electronic reorganization only happens around the Fermi energy, very little differences appear in the electron density and the electron localization function. Hence, we have focused in the region where the fractional occupation changes in order to understand the electronic structure. With this trick, we have been able to visualize the changes upon the set up of the superconducting state, as well as with respect to temperature. Whereas in H_3S the main differences appear along the stretching and bending directions, LaH_{10} main differences show up in a degeneracy in the H_4 region, which is boosted as temperature decreases. Since these directions could be related to the strong anharmonicity, it will be the aim of future work to analyze deformations along these directions. Overall, no important differences were observed in the values and positions of the critical points (unless direct focus at the Fermi level). This explains the ability of DFT (de)localization channels to reflect (de)localization in the superconducting state.

Acknowledgements

We would like to acknowledge support by ECOS-Sud C17E09 and C21E06, and the Association Nationale de la Recherche under grant ANR-22-CE50-0014. This research was supported by the European Research Council (ERC) under the European Unions Horizon 2020 research and innovation programme (grant agreement No. 810367), project EMC2. This work was performed using HPC resources from GENCI–IDRIS A0160915069 and A0160815101. CC acknowledges ANID for the grants ECOS210019 and FONDECYT 1220366, and the Center for the Development of Nanosciences and Nanotechnology, CEDENNA AFB 220001. W.M. acknowledges the support of ANID Chile through the Doctoral National Scholarship N° 21211501. Powered@NLHPC: This research was partially supported by the supercomputing infrastructure of the NLHPC (ECM-02)

References

(1) Drozdov, A. P.; Eremets, M. I.; Troyan, I. A.; Ksenofontov, V.; Shylin, S. I. Conventional superconductivity at 203 kelvin at high pressures in the sulfur hydride system. *Nature* **2015**, *525*, 73.

(2) Troyan, I. A. et al. Anomalous High-Temperature Superconductivity in YH6. *Advanced Materials* **2021**, *33*, 2006832.

(3) Drozdov, A.; Kong, P.; Minkov, V.; Besedin, S.; Kuzovnikov, M.; Mozaffari, S.; Balicas, L.; Balakirev, F.; Graf, D.; Prakapenka, V.; others Superconductivity at 250 K in lanthanum hydride under high pressures. *Nature* **2019**, *569*, 528–531.

(4) Kong, P.; Minkov, V. S.; Kuzovnikov, M. A.; Drozdov, A. P.; Besedin, S. P.; Mozaffari, S.; Balicas, L.; Balakirev, F. F.; Prakapenka, V. B.; Greenberg, E.; Eremets, M. I. Superconductivity up to 243 K in yttrium hydrides under high pressure. *Nature Communications* **2021**, *12*.

(5) Bardeen, J.; Cooper, L. N.; Schrieffer, J. R. Theory of Superconductivity. *Phys. Rev.* **1957**, *108*, 1175–1204.

(6) Eliashberg, G. M. Interactions between electrons and lattice vibrations in a superconductor. *Sov. Phys. - JETP (Engl. Transl.); (United States)* **1960**, *11*.

(7) Morel, P.; Anderson, P. W. Calculation of the Superconducting State Parameters with Retarded Electron-Phonon Interaction. *Phys. Rev.* **1962**, *125*, 1263–1271.

(8) Scalapino, D. J.; Schrieffer, J. R.; Wilkins, J. W. Strong-Coupling Superconductivity. I. *Phys. Rev.* **1966**, *148*, 263–279.

(9) Oliveira, L. N.; Gross, E. K. U.; Kohn, W. Density-Functional Theory for Superconductors. *Phys. Rev. Lett.* **1988**, *60*, 2430–2433.

(10) Oliveira, L. N.; Gross, E. K. U.; Kohn, W. Density-Functional Theory for Superconductors. *Phys. Rev. Lett.* **1988**, *60*, 2430–2433.

(11) Lüders, M.; Marques, M. A. L.; Lathiotakis, N. N.; Floris, A.; Profeta, G.; Fast, L.; Continenza, A.; Massidda, S.; Gross, E. K. U. Ab initio theory of superconductivity. I. Density functional formalism and approximate functionals. *Phys. Rev. B* **2005**, *72*, 024545.

(12) Sanna, A. In *Introduction to Superconducting Density Functional Theory*; Pavarini, E., Koch, E., Scalettar, R., Martin, R., Eds.; The Physics of Correlated Insulators, Metals, and Superconductors; Forschungszentrum Jülich, 2017; Vol. 7.

(13) Sanna, A.; Pellegrini, C.; Gross, E. K. U. Combining Eliashberg Theory with Density Functional Theory for the Accurate Prediction of Superconducting Transition Temperatures and Gap Functions. *Phys. Rev. Lett.* **2020**, *125*, 057001.

(14) Belli, F.; Novoa, T.; Contreras-García, J.; Errea, I. Strong correlation between electronic bonding network and critical temperature in hydrogen-based superconductors. *Nature Communications* **2021**, *12*, 1–11.

(15) Novoa, T.; di Mauro, M.; Errea, I.; Braïda, B.; Contreras-García, J. Molecularity: a fast and efficient criterion for probing superconductivity. *submitted*

(16) Becke, K. E., A. D.and Edgecombe A simple measure of electron localization in atomic and molecular systems. *J. Chem. Phys.* **1990**, *92*, 5397.

(17) Savin, A.; Nesper, R.; Wengert, S.; Fässler, T. F. ELF: The Electron Localization Function. *Angew. Chem. Int. Ed. Engl.* **1997**, *36*, 1808–1832.

(18) von Weizsäcker, C. F. Zur Theorie de Kernmassen. *Z. Phys.* **1935**, *96*, 431.

(19) Novoa, T.; Contreras-García, J.; Fuentealba, P.; Cárdenas, C. The Pauli principle and

the confinement of electron pairs in a double well: Aspects of electronic bonding under pressure. *The Journal of Chemical Physics* **2019**, *150*.

(20) Feixas, F.; Matito, E.; Duran, M.; Solà, M.; Silvi, B. Electron localization function at the correlated level: a natural orbital formulation. *Journal of chemical theory and computation* **2010**, *6*, 2736–2742.

(21) Echeverri, A.; Gallegos, M.; Gómez, T.; Pendás, A. M.; Cárdenas, C. Calculation of the ELF in the excited state with single-determinant methods. *The Journal of Chemical Physics* **2023**, *158*.

(22) Tinkham, M. *Introduction to Superconductivity*; International series in pure and applied physics; McGraw Hill, 1996.

(23) Kresse, G.; Hafner, J. Ab initio molecular dynamics for liquid metals. *Phys. Rev. B* **1993**, *47*, 558(R).

(24) Kresse, G.; Hafner, J. Ab initio molecular-dynamics simulation of the liquid-metal–amorphous-semiconductor transition in germanium. *Phys. Rev. B* **1994**, *49*, 14251.

(25) Kresse, G.; Furthmüller, J. Efficiency of ab-initio total energy calculations for metals and semiconductors using a plane-wave basis set. *Comput. Mater. Sci.* **1996**, *6*, 15.

(26) Kresse, G.; Furthmüller, J. Efficient iterative schemes for ab initio total-energy calculations using a plane-wave basis set. *Phys. Rev. B* **1996**, *54*, 11169.

(27) Perdew, J. P.; Burke, K.; Ernzerhof, M. Generalized Gradient Approximation Made Simple. *Phys. Rev. Lett.* **1996**, *77*, 3865–3868.

(28) Blöchl, P. E. Projector augmented-wave method. *Phys. Rev. B* **1994**, *50*, 17953–17979.

(29) Linscheid, A.; Sanna, A.; Floris, A.; Gross, E. K. U. First-Principles Calculation of the Real-Space Order Parameter and Condensation Energy Density in Phonon-Mediated Superconductors. *Phys. Rev. Lett.* **2015**, *115*, 097002.

(30) Drozdov, A. P.; Eremets, M. I.; Troyan, I. A.; Ksenofontov, V.; Shylin, S. I. Conventional superconductivity at 203 kelvin at high pressures in the sulfur hydride system. *Nature* **2015**, *525*, 73–76.

(31) Eremets, M. I.; Minkov, V. S.; Drozdov, A. P.; Kong, P. P.; Ksenofontov, V.; Shylin, S. I.; Budko, S. L.; Prozorov, R.; Balakirev, F. F.; Sun, D.; Mozaffari, S.; Balicas, L. High-Temperature Superconductivity in Hydrides: Experimental Evidence and Details. *Journal of Superconductivity and Novel Magnetism* **2022**, *35*, 965–977.

(32) Errea, I.; Calandra, M.; Pickard, C. J.; Nelson, J. R.; Needs, R. J.; Li, Y.; Liu, H.; Zhang, Y.; Ma, Y.; Mauri, F. Quantum hydrogen-bond symmetrization in the superconducting hydrogen sulfide system. *Nature* **2016**, *532*, 81–84.

(33) Bianco, R.; Errea, I.; Calandra, M.; Mauri, F. High-pressure phase diagram of hydrogen and deuterium sulfides from first principles: Structural and vibrational properties including quantum and anharmonic effects. *Phys. Rev. B* **2018**, *97*, 214101.

(34) Pendás, A. M.; Blanco, M. A.; Costales, A.; Sánchez, P. M.; Luaña, V. Non-nuclear Maxima of the Electron Density. *Phys. Rev. Lett.* **1999**, *83*, 1930–1933.

(35) Errea, I.; Calandra, M.; Pickard, C. J.; Nelson, J.; Needs, R. J.; Li, Y.; Liu, H.; Zhang, Y.; Ma, Y.; Mauri, F. High-Pressure Hydrogen Sulfide from First Principles: A Strongly Anharmonic Phonon-Mediated Superconductor. *Phys. Rev. Lett.* **2015**, *114*, 157004.

(36) Liu, H.; Naumov, I. I.; Hoffmann, R.; Ashcroft, N. W.; Hemley, R. J. Potential high-T(c) superconducting lanthanum and yttrium hydrides at high pressure. *Proc Natl Acad Sci U S A* **2017**, *114*, 6990–6995.